Geochemical and Geophysical Investigation
Southwest Ridge of Susie Mountain
Goodnews Bay Platinum Project
July - August, 2004

by:

Calista Corporation:
Jeff Foley - Senior Geologist
June McAtee - Vice President, Geologist
Michelle Pearson - GIS Geologist

Consulting Geologist:
W. I. Van der Poel

Contents

List of Figures

List of Plates (in pocket; scale 1:24,000)

List of Data (on CD in pocket)

\Goodnews_2004\Geochem

04GNB_grid_locations.xls	2004 Sample locations and data
04GNB_rock_Sample_Card_data.xls	in Excel tables and GIS shapefiles
04GNB_Soil_Sample_Card_data.xls	"
04GNB-rock-geochem.xls	"
04GNB-soil-geochem.xls	"
04GNB-rock-geochem_utm4nad27.shp	"
04GNB-soil-geochem_utm4nad27.shp	"
Rock Samples.xls	Previous geochem data from
Soil Samples.xls	master file Gnews DB 7-18-00.mdb
All_rocks.shp	"
All_soils.shp	"
Gnews DB 7-18-00.mdb	"

\Goodnews_2004\Geology

auger_cutting_geology.shp	points – auger cutting geology
geol04_polygons.shp	polygon – 04 geologic mapping
geol04_polygons.lyr	ArcGIS layer file – symbol settings
gnb_geol_lines_ver1.shp	polylines – 04 geologic mapping
geol04_lines.lyr	ArcGIS layer file – symbol settings
Serpentine Alteration.lyr	ArcGIS layer file – symbol settings

\Goodnews_2004\Geophysics\

04GNB-soil-sscept.xls	soil susceptibility data
04GNB-rock-sscept.xls	surface rock susceptibilities
gnbtfmag04.tif and .tfw	total field aeromag, log scale
CheckSurvey730corCompEd.xls	ground mag 04,UTM and grid coords
Survey730corCompEdbln.grd	Surfer grid, mag 04, UTM
MagUTMvsSuscept.srf	Surfer plot, mag 04 plus other data
GNW25s.wk1	resist and phase data, line 25S, Lotus
GNW26s.wk1	resist and phase data, line 26S, Lotus
SSZSoilPt25S.xls	Pt in soil, with elevations, 25S
SSZSoilPt26S.xls	Pt in soil, with elevations, 26S
SSZ25S.grd	Surfer grid, resist Line 25S
SSZ26S.grd	Surfer grid, resist Line 25S
SSZ2526S.srf	Surfer plot, resist and soils 25 & 26S

\Goodnews_2004\pdfs

- Susie Mtn Fig1_Location_map.pdf
- Susie Mtn Figure 2 2004 final rpt.pdf
- Susie Mtn Fig 3 magsus 2004 final rpt.pdf
- Susie Mtn Fig 4 profiles 2004 final rpt.pdf
- Plate 1 GNB 2004 final rpt.pdf
- Plate 2 GNB 2004 final rpt.pdf
- Plate 3 GNB 2004 final rpt.pdf

\Goodnews_2004\report

- 2004_GNB_report.doc
- 2004_GNB_report.pdf

Geochemical and Geophysical Investigation
Southwest Ridge of Susie Mountain
Goodnews Bay Platinum Project
July - August, 2004

Summary

During late July and early August, rock and soil geochemical samples, total field magnetic, magnetic susceptibility and resistivity data were collected on the southwest ridge of Susie Mountain. The data were collected on a portion of the Susie Mountain grid where anomalous platinum content was previously detected in surface rocks and airborne data indicate a ridge in the magnetic field. The geochemical data confirm concentrations of platinum (Pt) in the area, with one rock sample containing 2.5 ppm Pt and elevated concentrations in soil samples. However, the data do not indicate a coherent zone of ore grade material near the surface.

Elevated Pt values in rock and soil are concentrated in a zone of olivine clinopyroxenite and serpentinized peridotite in the southwest third of the study area and along the margins of an arcuate magnetic high associated with strongly serpentinized peridotite and high resistivities on the ridge crest. Overall, the magnetic data show an arcuate and concentric pattern, suggestive of diapiric emplacement of adjacent or underlying portions of the complex and coeval to post-emplacement hydrothermal alteration and serpentinization.

Whereas Pt concentrations do not correlate well numerically with geophysical parameters, they do appear to be associated with complex signatures which suggest structural and lithological influences as well as alteration. The aggregate of the data indicate additional exploration for deeper targets is warranted in the context of a comprehensive exploration program.

Background

A review of raw data provided to Calista by lessors of the property indicated an area on the southwest ridge of Susie Mountain (Figure 1) had yielded anomalous Pt values from surface rock samples. CSAMT data further north on the ridge indicated a resistivity low at depth, similar to more extensive features noted on Red Mountain. The combination of these factors indicated this area warranted further definition of the potential for near-surface mineralization as well as deeper targets.

Methods

The field effort crossed the area of interest with eight lines, 100 meters apart, on which stations were flagged at 20-meter intervals with supplementary lathe and flagging positioned at 100-meter intervals. The grid was extended from monuments of a local grid established on Susie Mountain in 1994. Rock chip and soil auger samples were collected at 20-meter intervals and the total magnetic field was measured by a ground survey at 10-meter intervals. Field data for soil and rock chip sampling were entered into *IPAQ* hand-

held computers in the field using *Pocket PC Creations* software and later downloaded to *Microsoft Excell* spreadsheet files. Magnetic susceptibilities of all samples were measured in the bags and a ground susceptibility survey was performed on rubble and outcrop within the project area using GPS control. Magnetotelluric (MT)-type resistivity at VLF (VLF-R) was measured on two lines in the central portion of the grid.

Surveying: Initial attempts to extend the earlier grid by compass and string box methods gave unacceptable results due to the strong magnetic field in the area which produced foresight/backsight errors of more than three degrees. As a result, hand held GPS units (*Garmin 12XL and 60C*) were used to establish the lines and stations. Because there is an inherent 3- to 6-meter instrumental error, some of the lines show locally erratic station to station placement, however this method appears to have produced good consistency and recoverability when considered in the context of the grid as a whole. Actual sample collection points were locally displaced from surveyed stations due to soil or rock conditions and these points were recorded with *Holux* GPS units attached to the hand-held computers. Agreement between the various GPS units appeared to be within the 3- to 6-meter errors indicated by the *Garmin* units.

Data are plotted on a base map in the NAD27 Datum to allow comparison with earlier data sets (Figures 2 - 3 and Plates 1 - 3). Becuase there are numerous algorithms for estimating NAD27 coordinates from primary GPS readings, there are minor inconsistencies with data collected prior to this effort where different instruments and software were used. For example, coordinates derived from the *Trimble* "Seven parameter" algorithm in 1996, used for the gravity survey, are approximately 12 meters from the same points plotted with data from the Garmin units. These inconsistencies do not appear to have negatively affected the work this season.

Geologic Mapping: A detailed geologic map (Figure 2-A) was compiled on the basis of the relative abundance of various rock types observed in frost-riven float, rubble, soil auger cuttings and minimal exposed bedrock. Because bedrock is exposed in less than 1 percent of the area and all other material is subject to frost heave, solifluction and other processes that result in downslope transport and mixing, the map is merely a best effort to interpret primary lithologic distribution at the surface and in the shallow subsurface. Mapping is further complicated by the relative abundance of olivine in all lithologies and an almost complete gradation of pyroxene content in the various rocks. In addition to mapping major lithologic distribution, attention was paid to primary rock fabric, minor mineral content and degree of serpentinization and other alteration and secondary mineral products.

Rock Geochemistry: Rock sampling (Figure 2-A) attempted to collect representative suites of chips in the pebble-to-outcrop size range within a 5-meter radius of the flagged stations. Samples were not collected where suitable materials were absent and as a result the distribution of rock chip samples is less extensive than the soil samples or the geophysical data.

Rock samples were analyzed by *ALS Chemex*, using a 47-element ICP-MS method,

following crushing and multi-acid digestion. Gold, platinum and palladium were analyzed by combined fire assay AA-ICP procedure on 30-gram sample splits.

Class intervals for Pt in rock samples in Figure 2-A were arbitrarily selected to distinguish samples with significantly higher Pt concentrations

Soil Geochemistry: Soil samples (Figure 2-B) were collected with a gasoline-powered auger using a single auger flight, 2 inches in diameter and 1.6 meters long. Samples were collected from the greatest depth practical, generally greater than one meter. The sampling process often required 3 - 8 holes to collect sufficient sample volume. In most cases, this method allowed samplers to collect weathered bedrock material from beneath brown, clayey silt surface deposits. In some cases, particularly on the flanks of the ridge where the surface deposit was thicker than near the ridge crest, it is inferred that the sample material represents the mass wasting surface deposit. Whether the parent material was near-source bedrock or transported silt-clay soil from a solifluction terrace, most of the sampled material appeared to be derived from the C soil horizon (Cox). Database and spreadsheet files on the CD in the "Data" appendix, provide detailed information on all samples.

Soil samples were analyzed by *ALS Chemex*, using a 47-element ICP-MS method, following screening to minus 80 mesh and multi-acid digestion. Gold, platinum and palladium were analyzed by combined fire assay AA-ICP procedure on 30-gram sample splits. Class intervals for Pt in soil samples in Figures 3-B were chosen to best show the range and distribution of anomalous concentrations.

Magnetic Field Measurements: Measurements of the total magnetic field (Figure 2B) were made at 10-meter intervals along the flagged lines with a *Geometrics 856* proton precession magnetometer, configured to 1 gamma sensitivity. The locations of points (10-meter station intervals) between flagged stations (20-meter intervals) were estimated by eye and are considered to be within 1 or 2 meters of their nominal location. The UTM coordinates of the magnetic stations were digitized by overlaying a Cartesian grid of the survey area on the plotted GPS locations of samples, then shifting the grid for best fit.

Due to the extremely high local variance caused by magnetite content in bedrock, a recording base was not used. To reduce the influence of diurnal drift, the operator regularly re-occupied grid station -2200, -100 (22S, 1W) and obtained repeat readings. The extreme variance at this station was 36 gammas, confirming that drift was insignificant with respect to the overall data set. Nonetheless, synthetic base station files were constructed using the repeat readings and the data were corrected for drift using *Geometric's Mag Map* software, assuming a nominal base station value of 53,905 gammas. Prior to final compilation, selected, high-gradient spikes were cleaned from the data. Experiments with filtering and plotting gradients indicated these added little useful information and are not included in the report.

Magnetic Susceptibility Measurements: Magnetic susceptibility measurements were obtained in SI units using a *SM30* susceptibility meter manufactured by *ZH Instruments*.

Surface rock susceptibilities were measured at stations distributed throughout the study area where suitable materials were available. At most stations, the operator recorded the susceptibilities of five rocks, including float, rubble and outcrop, which appeared to be representative of the area within 5 meters (Figure 3A). GPS coordinates were obtained at each of these stations.

Measurements were obtained on all rock and soil samples in their bags. Measurements averaged at least two readings on different sides of the bags, and for high variance samples, three to five readings were averaged. Due to the high variance of bagged rock samples, these values are not presented in graphic summary. The susceptibilities of bagged soil samples (Figure 3B) were found to be reproducible to within roughly 10 percent.

Resistivity: Magnetotelluric-type resistivity and phase data at VLF (Very Low Frequency; VLFR) were collected on lines 2500 and 2600 South (-2500, -2600) using a *Geonics EM16R*, tuned to the transmitter near Jim Creek, WA (NLK) (Figure 4). The data were reduced to modeled sections using *Griessman and Reitmayr's 1-D inversion algorithm*, as provided by the instrument manufacturer.

Results

Rock Geochemistry: Platinum in rock is erratically concentrated along the ridge crest, generally in the northeast, south and southwest portions of the grid (Figure 2-A). While the magnitude and distribution of high Pt samples generally confirms the results of earlier, less controlled sampling, it does not suggest a concentration of ore grade rock near surface. In relation to the other data sets, spatial correlation appears to be moderate with soil geochemistry, and weak-to moderate with magnetic field and susceptibility. Platinum is elevated in rocks near the margins of the magnetic ridge in the central portion of the study area and to a lesser degree in the southwest third of the grid. That area is characterized by mid-range magnetic response with relatively low variance. Resistivity data appear to show moderate correlation between the margins of the resistivity high, steep gradients and high Pt content in nearby rocks. The small volume of resistivity data limits the conclusions which can be drawn from it.

Soil Geochemistry: Platinum distribution in soil (Figure 2-B) shows a moderate spatial similarity to the distribution of Pt in rocks but varies notably in having lower variance and a more coherent concentration in the southwest third of the grid. That area corresponds most closely to an area dominated by olivine clinopyroxenite in float and in auger samples. It is bounded abruptly on the southeast margin by a discontinuity in magnetic and resistivity data which are inferred to indicate a fault close to the grid base line (0E). To the north and northeast, the boundary generally coincides with an arcuate magnetic high on the ridge crest.

The soil data depart dramatically from the results of earlier, more surficial soil sampling, confirming that the greater depth achieved with the powered auger is more effective at detecting Pt concentrations.

Geologic Mapping and Interpretation: Geologic mapping in the Goodnews Bay ultramafic complex by Alaska Earth Sciences (AES) and Southworth (1986) shows a well-developed concentric distribution of major lithologies at Red and Susie Mountains (Plates 1 and 2). In both massifs, dunite is central to surrounding clinopyroxene-rich lithologies, including peridotite (wehrlite), olivine clinopyroxenite, magnetite clinopyroxenite and hornblende clinopyroxenite. At Red Mountain, dunite is much more abundant than at Susie Mountain, which comprises predominately peridotite and olivine clinopyroxenite with minor dunite. It has been suggested that this reflects a deeper level of erosion at Red Mountain than at Susie Mountain, where dunite is less extensive than peridotite.

Within the small area investigated at Susie Mountain in 2004, peridotite and olivine clinopyroxenite are the two most abundant primary lithologies (Figure 2-A). Small dunite and mixed dunite/peridotite outcrop, rubblecrop, and scattered dunite float are variably present within more abundant peridotite rubble and float along the ridge. Olivine clinopyroxenite segregations, dikes and sills, as much as a meter thick, are common within the peridotite-dunite body. Olivine clinopyroxenite and relatively monomineralic clinopyroxenite underlie the areas to the west, south and east of the ridge crest.

Earlier mapping by AES shows a NNE-striking fault separating the peridotite and clinopyroxenite masses at the southwest end of Susie Mountain (Plates 1 and 2). The NNE fault intersects a NE-striking fault farther up the ridge from the 2004 area of sampling and geophysical surveys. Pronounced shearing, serpentinization and a slump feature mapped during this investigation along the west side of the ridge are consistent with the presence of the NNE fault zone as mapped by AES. An elongate area along the central ridge shown in figure 2-A, and measuring from 80 to 150 meters wide, is distinguished by an abundance of green and black, talcose, sheared and serpentinized ultramafic float intermixed with less altered peridotite and less abundant olivine clinopyroxenite and dunite. Within this central disrupted zone, ultramafic rocks tend to have a sheared and granular fabric compared to a better-preserved, massive hobnail texture in peridotite outside the zone where resistant pyroxene protrudes from more recessive, dun-weathering olivine-rich groundmass.

Figure 2-A shows that the serpentinized and disrupted zone roughly coincides with the extent of granular peridotite and dunite. Alternative explanations are offered for the coincidence of these features. On the one hand, the serpentinization and associated structural event may have been confined to the peridotite mass or its margins, possibly because of a difference in competence between the peridotite and clinopyroxene rich rocks. Alternatively, the fluids and disruption that occurred within the peridotite and along the faulted western contact with the clinopyroxenite may have also penetrated the clinopyroxenite mass, which is very poorly exposed. Olivine, the predominate mineral present in peridotite, would react more readily with serpentinizing fluids to form talc, chrysotile, antigorite and magnetite, which are all common in the mapped area. Clinopyroxene, on the other hand, is less susceptible to serpentinization and would not as

readily show the effects of the altering fluids. In addition, because clinopyroxenite is mostly observed in float and rubble along the ridge flanks and in auger cuttings from beneath vegetation and surficial deposits, it is difficult to ascertain the effects of a serpentinizing event that might have affected it.

At several sites within and marginal to the serpentinized zone, additional alteration effects are observed. Where serpentinized peridotite is cut by very fine, 0.5-3.0 mm cross-fiber chrysotile veinlets and vein networks, the rocks typically contain abundant disseminated calcite with a sugary texture, and rarely, finely disseminated iron and iron-copper sulfide minerals. Fine-grained magnetite is ubiquitous in both the serpentinized and relatively less altered peridotites. More rarely, coarse interstitial magnetite is observed, particularly in association with hornblende that is locally very coarse grained or massive. At half a dozen or more sites, accessory coarse-grained flakes of brown to black mica (phlogopite-biotite) were observed in altered peridotite and olivine clinopyroxenite.

Elevated Pt concentrations are not confined to a specific rock type or mineral association so far identified at the southwest ridge of Susie Mountain. Among the 18 rock samples collected in 2004 that contain greater than 0.050 ppm Pt (Table 1), are a mix of serpentinized peridotite, olivine clinopyroxenite and dunite with various accessory, trace and alteration mineral assemblages including chromite, magnetite, hornblende, mica, asbestos, mica and calcite. Whereas very fine-grained trace iron and iron-copper sulfide minerals were observed in a few rock samples, in particular those cut by cross fiber asbestos veinlets, sulfides were observed in none of the samples listed in Table 1 and do not appear to correlate with the higher observed Pt values. A possible exception to this observation is 04GNB466 which was partially coated with red-orange iron-oxide and contains boxwork weathering pits, possibly after weathered sulfide minerals.

Table 1. Selected analytical results and rock chip sample descriptions for samples containing greater than 0.050 ppm Pt, Susie Mountain, 2004

SAMPLE	Pt(ppm)	Pd(ppm)	Sample Description
04GNB480	2.520	0.061	Serpentinized dunite with accessory disseminated chromite
04GNB413	1.820	0.059	80 pct olivine clinopyroxenite and 20 pct serpentinized peridotite
04GNB433	0.311	0.007	Serpentinized peridotite with minor orange-weathering, talcose hornblende olivine clinopyroxenite
04GNB364	0.180	0.006	Equal mix of serpentinized peridotite and olivine clinopyroxenite with cross-fiber asbestos veinlets
04GNB343	0.177	0.004	Serpentinized peridotite
04GNB455	0.162	0.004	Mixture of serpentinized peridotite and olivine clinopyroxenite
04GNB466	0.150	0.002	Serpentinized peridotite and minor olivine clinopyroxenite with red-orange weathering boxworks
04GNB366	0.136	0.004	Serpentinized olivine clinopyroxenite with brown olivine and accessory brown mica
04GNB440	0.118	0.003	Serpentinized peridotite with milky clinopyroxene veinlets and accessory chromite
04GNB334	0.114	0.001	Serpentinized peridotite
04GNB368	0.105	0.004	Olivine clinopyroxenite and minor serpentinized peridotite
04GNB367	0.104	0.003	Olivine clinopyroxenite
04GNB414	0.086	0.005	Olivine clinopyroxenite and minor serpentinized peridotite
04GNB311	0.078	0.003	Mixture of serpentinized peridotite and olivine clinopyroxenite
04GNB304	0.072	0.002	Serpentinized peridotite with minor dunite
04GNB472	0.067	0.003	Equal mix of serpentinized peridotite and olivine clinopyroxenite
04GNB473	0.065	0.002	Olivine clinopyroxenite and minor serpentinized peridotite
04GNB303	0.061	0.004	Mixture of serpentinized peridotite and olivine clinopyroxenite

Given that mineralization, as detected in rock and soil samples from the area is concentrated within an area characterized by the presence of both peridotite and clinopyroxenite, and is further characterized by structural deformation and chemical alteration, the possibility of the serpentinizing event influencing said mineralization must be considered. Furthermore, we suggest that elevated Pt concentrations along Susie Ridge may be the result of a late-stage dunite-peridotite intrusive event and associated fluids being intruded into the already zoned complex.

Total Magnetic Field: Although the local magnetic field measured by the ground survey this season is generally consistent with features in the aeromagnetic data, the ground data provide greater detail and are more strongly influenced by smaller bodies near the surface with shorter response wavelengths (Figure 2-A). In some cases, field readings were influenced by extremely high gradients from magnetite-rich boulders on the surface. Another factor which may influence the total magnetic field is the presence of zones of reversed polarity remanent magnetism, recognized at both Red and Susie Mountains in earlier work. No measurements of remanent magnetism were undertaken for this phase of the investigation.

The magnetic data show an arcuate high along the ridge in the center of the study area and another high in a concentric configuration to the northeast, beneath colluvial deposits on the slopes facing Susie Creek. The highest magnetic response on the ridge generally coincides with rubble of moderately to highly serpentinized peridotite and dunite, though at the surface, lithologic boundaries crosscut the magnetic features. In the southwest portion of the grid, a zone of mid-level magnetic response and low variance is associated with olivine clinopyroxenite. Near the baseline (0E) on lines 25S, 26S and 27S, an abrupt gradient in the magnetic response corresponds to discontinuities in geochemical and resistivity data and is inferred to represent a fault.

While earlier work recognized a positive spatial correlation between platinum and elevated magnetic response in airborne magnetic data, the more detailed ground magnetic data collected this season show only an indirect correlation with mineralization. In the southwestern half of the grid, it appears that platinum is concentrated along the margins of the arcuate magnetic high on the ridge, and in the area of mid-range magnetic response associated with olivine clinopyroxenite. These associations suggest that while the numeric correlation with platinum content is poor, the genesis of the magnetic features and the concentration of Pt have common factors that are not yet recognized.

The total magnetic field shows a reasonably good spatial correlation with magnetic susceptibility measurements in soil, and a somewhat weaker but positive correlation with susceptibilities in rocks (Figures 2-A, 3-A and 3-B). It is notable that soil samples show elevated susceptibilities that persist downslope from their counterparts in the magnetic field along the ridge crest. If the magnetic lows on the flanks of the ridge are due to reduced magnetite content and not polarity reversals, the downslope dispersion of magnetite suggests solifluction and mass wasting processes have moved a mantle of surface material at least 200 meters away from its source. This observation should be considered when evaluating float mapping and geochemical sampling in the project area since it suggests the extent of core-type lithologies such as peridotite and dunite may be exaggerated.

Magnetic Susceptibility: It has long been recognized that placer concentrates at Goodnews Bay are magnetic, and that magnetic concentrates are platiniferous. In earlier drilling on Red Mountain, drill core from rock underlying anomalous soil platinum showed erratic but elevated susceptibilities. The work this season, however, found poor numeric correlation between platinum in soil and magnetic susceptibility ($r = .089$).

Magnetic susceptibilities in soil are elevated along the ridge crest and the southeast slope of the ridge in areas dominated by a mixture of variably serpentinized peridotite, dunite and other minor rock types (Figure 3B). This distribution correlates reasonably well with the total magnetic field. Several stages of serpentinite-related magnetite can be recognized, as well as cumulus and contact metamorphic variants, though it is not clear what the genetic relationship between one or more of the types of magnetite and platinum may be. Comments under "Total Magnetic Field" (above), address the relationship between susceptibility and that parameter.

Resistivity: The two resistivity profiles show generally resistive rock materials with a low-over-high resistivity section (Figures 4-A and 4-B). In both profiles, low resistivity surface deposits, represented by warmer colors, are seen thickening away from the ridge crest. More resistive rocks underlie the ridge on both profiles, roughly from 1W to 2W (-100 to -200). This zone is associated with rubble of pervasively serpentinized peridotite and dunite. Inspection of the magnetic data also shows that this zone corresponds reasonably well to the arcuate magnetic high along the ridge crest.

Dots representing Pt in soil have been plotted along the surface of each profile using pseudologarithmic binning intervals. These appear to show a tendency toward higher values on the margin of the resistive and magnetic signature associated with zone of strong serpentinization. These areas are also characterized by a moderately strong suggestion of vertical structures, perhaps representing steeply dipping faults or local contacts. It is noteworthy that the strong high-over-low resistivity signature on the southeast portion of line 26S is associated with distinctly lower Pt values.

Conclusions and Recommendations. While the data do not define a compelling near surface Pt concentration, the spatial relationships between the geophysical and geochemical data are similar to those at Red Mountain, suggesting a common structural genesis and a potential for the system to be more prospective at depth. The apparent concentration of platinum near the margins of the serpentinized zone, delineated as magnetic and resistivity highs, could be consistent with a “roll front” style of platinum remobilization during late stage, hydrous phases of intrusion. Elevated Pt values in olivine clinopyroxenite indicate a localized enrichment in differentiated border phases of the complex which could achieve greater concentrations elsewhere. In addition, the arcuate and concentric pattern to the total magnetic field data suggests fracture consistent with diapiric emplacement of a late intrusive phase. In aggregate, the data support essential criteria of differentiation, concentration and a permissive structural environment. Additional work is indicated to understand the deeper structure and potential for stronger mineralization.

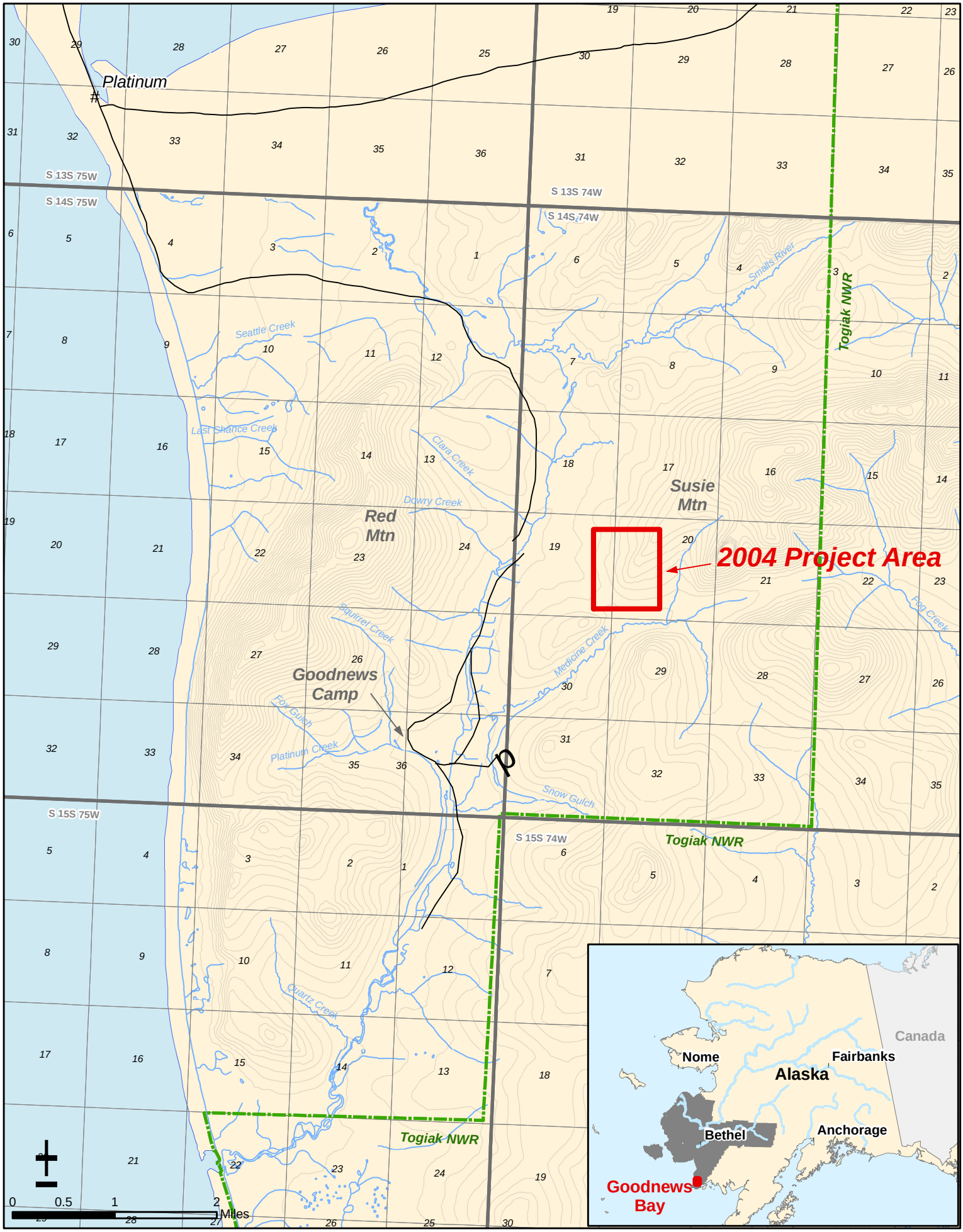

Figure 1: 2004 Goodnews Bay Project Location